Structure-based redesign of an edema toxin inhibitor

Deliang Chen [a], Lili Ma [b], John J. Kanalas [c], Jian Gao [c], Jennifer Pawlik [d,e], Maria Estrella Jimenez [b], Mary A. Walter [c], Johnny W. Peterson [d,e], Scott R. Gilbertson [b], Catherine H. Schein [a,d,e,f,*]

[a] Sealy Center for Structural Biology and Molecular Biophysics, Department of Biochemistry and Molecular Biology, UTMB, Galveston, TX 77555-0857, USA
[b] Department of Chemistry, University of Houston, Houston, TX 77004, USA
[c] Mission Pharmacal Company, San Antonio, TX, USA
[d] Sealy Center for Vaccine Development, Center for Biodefense and Emerging Infections, UTMB, Galveston, TX 77555, USA
[e] Department of Microbiology and Immunology, UTMB, Galveston, TX 77555-1070, USA
[f] Institute for Translational Studies, UTMB, USA

ARTICLE INFO

ABSTRACT

Edema factor (EF) toxin of *Bacillus anthracis* (NIAID category A), and several other toxins from NIAID category B Biodefense target bacteria are adenylyl cyclases or adenylyl cyclase agonists that catalyze the conversion of ATP to 3′,5′-cyclic adenosine monophosphate (cAMP). We previously identified compound **1** (3-[(9-oxo-9H-fluorene-1-carbonyl)-amino]-benzoic acid), that inhibits EF activity in cultured mammalian cells, and reduces diarrhea caused by enterotoxigenic *Escherichia coli* (ETEC) at an oral dosage of 15 μg/mouse. Here, molecular docking was used to predict improvements in potency and solubility of new derivatives of compound **1** in inhibiting edema toxin (ET)-catalyzed stimulation of cyclic AMP production in murine monocyte-macrophage cells (RAW 264.7). Structure–activity relationship (SAR) analysis of the bioassay results for 22 compounds indicated positions important for activity. Several derivatives demonstrated superior pharmacological properties compared to our initial lead compound, and are promising candidates to treat anthrax infections and diarrheal diseases induced by toxin-producing bacteria.

1. Introduction

The toxins produced by many pathogenic bacteria cause morbidity and mortality in infected individuals. For example, the toxins of *Bacillus anthracis*, a naturally occurring pathogen that has been used as a bioweapon,[1] are important virulence factors. The toxin complex consists of two classic AB toxins, where enzymatic moiety A is either a Zn^{2+} metalloprotease, lethal factor (LF), or an adenylyl cyclase, edema factor (EF). Both enzymes require a "B" protein, protective antigen (PA), for receptor binding and cell entry[2]; combining PA and EF gives edema toxin (ET). Other groups have focused on inhibiting the interaction between EF and activators to control its activity.[3,4] We have focused on identifying non-nucleotide inhibitors that should bind to the active site of EF. These could be used together with LF inhibitors to treat late stage anthrax infections, where antibiotics might be unable to prevent death. These EF inhibitors could also be useful against pathogens which produce similar toxins, such as *Bordetella pertussis*, the causative agent of whooping cough.

Of three initial 'hits', we identified a novel inhibitor of EF, compound **1**[30] (Fig. 1), by using a combination of pharmacophore-based compound selection, molecular docking, and experimental screening with a cell-based bioassay.[5,6] Compound **1** consistently inhibited cAMP production induced by edema toxin (IC_{50} 2–9 μM in cells).[7] Compound **1** also reduced diarrhea caused by enterotoxigenic *Escherichia coli* (ETEC), at an oral gavage dose of 15 μg/mouse.[8] As we have previously shown that compound **1** inhibits cholera toxin,[9] which is 80% identical to lethal toxin of ETEC,[10] and human ETEC strains can also produce adenylyl cyclase toxins,[11] we attribute this activity to direct inhibition of the *E. coli* toxins. The ETEC study also suggested that the compound was working as an inhibitor of quorum sensing, which in many bacteria is controlled by cAMP levels[12,13], as the levels of bacteria in the colons of the infected and treated mice were much lower than those who did not receive the compound.

Here we describe the search for derivatives of Compound **1** that would have similar or better activity, with improved predicted aqueous solubility and reduced predicted toxicity. Compound **1** treatment gave no obvious toxic effect in the cell cultures or mouse studies, and the Ames II™ Mutagenicity Assay determined the compound **1** to be non-mutagenic in all conditions tested. However, there was a positive response for genotoxicity in the GreenScreen HC [GADD45α (growth arrest and DNA damage gene)-Green Fluorescent Protein (GFP)] assay test on mammalian cells (Supplementary Fig. 1 and Table 1) at 10–20× the active dose

* Corresponding author.
E-mail address: chschein@utmb.edu (C.H. Schein).
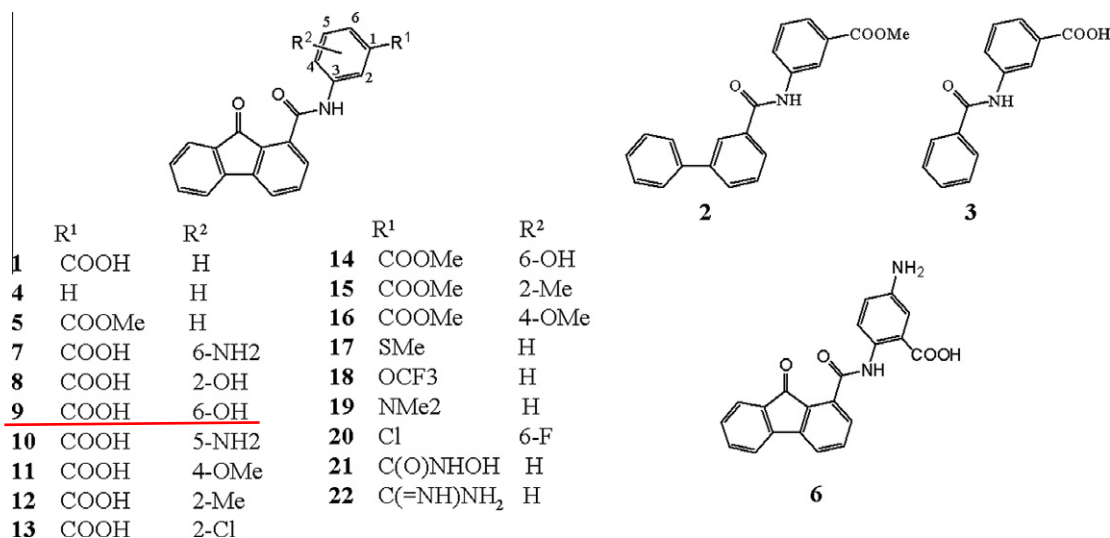
Figure 1. Structures for the lead compound **1** and derivatives **2–22** analyzed in this work.

Table 1
Values for the activity of the derivatives of compound **1** (Fig. 1) in inhibiting EF induced secretion of cAMP by cultured cells, compared to their $c\text{Log}P$, binding (BE) and docking energies (DE) calculated with Autodock.

Compound	R^1=	R^2=	$c\text{Log}P$	IC$_{50}$ (μM)		AutoDock scores	
				Assay 1[a]	Assay 2[a]	BE	DE
1	**–COOH**	**H**	**4.29**	**1.64–12.25 μM (many assays)**		**–13.28**	**–14.75**
2	See Figure 1		4.72	19.0 (±2.27)		–11.94	–11.86
3	See Figure 1		2.59	>100		–11.60	–11.53
4	H	H	4.77	28.6 (±2.97)		–11.72	–11.87
5	–COOMe	H	4.75	11.0 (±3.05)		–12.80	–13.19
6	See Figure 1		3.57	80.00 (±3.05)		–14.45	–14.97
7	–COOH	6-NH$_2$	3.57	6.08 (±3.09)		–14.28	–15.6
8	–COOH	2-OH	3.99	5.64 (±4.84)	5.64 (±5.99)	–14.11	–15.47
9	–COOH	6-OH	3.99	6.21 (±2.86)	6.21 (±2.86)	–14.53	–15.7
10	**–COOH**	**5-NH$_2$**	**3.57**	**1.30 (±0.23)**		**–14.34**	**–15.53**
11	–COOH	4-OMe	4.19	5.81 (±1.60)		–14	–15.3
12	–COOH	2-Me	4.61	11.36 (±8.55)	11.36 (±0.45)	–13.73	–15.46
13	–COOH	2-Cl	4.91	9.21 (±1.14)		–13.59	–15.18
14	–COOMe	6-OH	4.45	>100 (±2.11)	248.8 (±2.68)	–11.39	–12.91
15	–COOMe	2-Me	5.06	12.98 (±2.65)	12.92 (±2.65)	–11.46	–13.12
16	–COOMe	4-OMe	4.64	7.18 (±0.93)		–10.95	–12.65
17	–SMe	H	5.27	26.03 (±1.49)		–11.08	–11.88
18	–OCF$_3$	H	5.60	6.80 (±0.56)	6.86 (±1.33)	–10.69	–11.42
19	**–NMe$_2$**	**H**	**4.77**	**1.51 (±2.11)**	**1.51 (±0.46)**	**–10.66**	**–11.97**
20	–Cl	6-F	5.45	3.80 (±2.81)		–10.99	–11.78
21	–C(O)NHOH	H		12.92 (±4.94)		–13.15	–13.10
22	**–C(=NH)NH$_2$**	**H**	**3.15**	**2.71 (±0.83)**	**2.71 (±5.29)**	**–12.21**	**–13.34**

The most active compounds are given in bold type.
  [a] Assays were repeated for compounds that had IC$_{50}$ <20 μM in the initial assay, or where the results were not consistent with theory. The Descriptive Statics function in SigmaPlot was used to calculate STD Error for the data points closes to the IC$_{50}$ concentration.

(62.5 μg/ml vs active dose in mice of about 3 μg/ml, assuming 5 ml serum/mouse). Further, the $c\text{Log}P$ of compound **1** was high (4.29), it had to be dissolved in DMSO and then diluted into buffer 1:100 fold before adding to cell assays or for gavage. As the results here show, we were able to identify several derivatives with better predicted pharmaceutical properties, and equivalent or better activity in the bioassay for cAMP production induced by treatment of mammalian cells with ET.

2. Results

Derivatives of compound **1** were designed to add substituents at positions that had contact with residues important in the active site, according to docked conformations (Fig. 1 and Table 1). The

designed compounds were then redocked with AutoDock 3.0.[14,15] Our previous studies[5] indicated that the docking of 3d′ATP to the crystal structure of EF (PDB structure:1K90[16]) had low RMSD (root-mean-square deviations) between the predicted structure and the crystal structure, and thus, AutoDock 3.0 was reliable enough to predict the binding mode of the ligands to EF. The synthesized derivatives were dissolved in DMSO and then diluted at least 100-fold into cell culture medium. Their ability to reduce total extracellular cAMP production in mammalian cells treated with protective antigen (PA) and EF (which together[17] are called edema toxin, ET) was determined. This assay gives more variability than using isolated enzymes, but it is biologically relevant, as the concentrations needed to inhibit diarrhea and intestinal damage in the ETEC murine model (7.5–15 μg/mouse) were similar to those
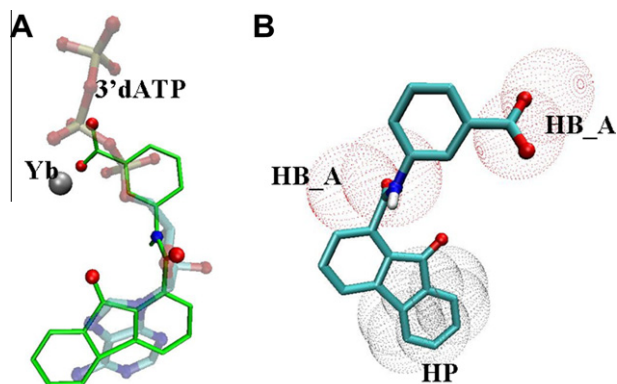
Figure 2. Overlay of the docked conformation of **1** A: with the position of 3d′-ATP in the crystal structure (in 1K90.pdb) and B: with the fragments of the original pharmacophore (dotted spheres) used to screen the ZINC database.[6]

indicated by the cell culture IC_{50} values for compound **1**.[8] The IC_{50} values for compound **1** in the assays shown here (Table 1) ranged from 1.64–12.6 μM, in part due to dilutions being done in 10-fold steps when large groups of inhibitors were assayed together. Assays were done in triplicate and samples with IC_{50} values <20 μM were assayed at least twice on different days, and re-assayed in two-fold dilution steps to reduce errors at lower doses. Below we summarize the key points of our structure–activity relationship analysis of these results.

2.1. The fluorenone ring and benzoic acid were essential for the activity of 1

Compounds **2–5** (Fig 1) were synthesized for the following reasons: **2**: reduce the fluorenone ring to a dibenzene (remove the carbonyl group) and change the carboxyl group to methyl ester; **3**: reduce the fluorenone ring to a benzene; **4**: remove the carboxyl group of the benzoic acid; and **5** (and others): change this carboxyl group to a methyl ester. The IC_{50} for compounds **2–5** were all higher than those for **1** (Table 1). Assay results for compounds **2** and **3** (as well as for other compounds that are not shown) indicated the fluorenone ring (which overlays the position of the purine ring of the ATP analogue in our dockings) was important for activity. Thus the bulk of our derivative study concentrated on alterations to the benzoic acid moiety. We also do not anticipate toxicity from this moiety, as the fluorenone itself in the interferon inducer tilorone[18] and related compounds[19] showed no toxic effects in cells.

Comparing compounds **4** and **5** it is clear that removing the carboxyl group of **1** had a more drastic effect on activity than changing it to a methyl ester. The overall decrease in activity was consistent with docking results that indicated this carboxyl overlaid the position of the α-phosphate of ATP from the crystal structure[16] and the negatively charged oxygen atom interacted with the metal ion to form an ion–ion interaction (Fig 2A). Our previous dockings indicated that the interaction with metal is the most important hydrogen bond or ion–ion interaction (Fig 2B).[5,6]

With these initial results in mind, further redesign concentrated on modifying the benzoic acid to increase the hydrogen bond interactions and/or the ion–ion interactions. Compounds **6–22** added substituents to the benzoic acid ring or replaced the carboxyl group of the benzoic acid with other groups. All the derivatives synthesized, compared to compound **1**, had lower calculated Log*P* (*c*Log*P*) values (Table 1), and most had lower expected toxicities, according to the on-line program OSIRIS Property Explorer (http://www.organic-chemistry.org/prog) (Table 2). With a few exceptions, any changes to **1** reduced potency, for reasons that could be explained by comparing docked conformations.

Table 2
Predicted toxicities (based on results from the on-line program OSIRIS Property Explorer)

Compound	Expected toxicity			
	Mutagenic	Tumorigenic	Irritant	Reproduct
1	**High**	**Low**	**Mid**	**Low**
2	Mid	Low	Low	Low
3	High	Low	Mid	Low
4	Low	Low	Low	Low
5	Low	Low	Low	Low
6	Low	Low	High	Low
7	High	High	Mid	Low
8	Low	Low	Low	Low
9	Low	Low	Low	Low
10	**High**	**Low**	**Mid**	**Low**
11	Mid	Low	Low	Low
12	Low	Low	Low	Low
13	Low	Low	Low	Low
14	Low	Low	Low	Low
15	Low	Low	Low	Low
16	Low	Low	Low	Low
17	Low	Low	Low	Low
18	Low	Low	Low	Low
19	**High**	**Low**	**High**	**Low**
20	Low	Low	Low	Low
21	Mid	Low	Low	Low
22	**Low**	**Low**	**Low**	**Low**

The most active compounds in Table 1 are given in bold type. None of the compounds were obviously toxic in the cell culture assay when added alone, at the highest dose tested.

2.2. The position of the carboxyl group

Moving the carboxyl group to any other position reduced activity, as shown, for example, by a much higher IC_{50} for **6** than for **7**. This was also consistent with docking results, where the binding affinity of **6** was lower than **7**. The docked structures suggested one explanation for this: the angle of the carboxyl of **6** to the metal ion deviated greatly from ideal geometry (88° versus the optimal hydrogen bond angle of $\geqslant 120°$[20,21] for the sp^2 oxygen atom; the angles for **1** and **7** are 121.5° and 117°, respectively).

2.3. Additions to the benzoic acid

Depending on their position, addition of hydrophilic groups such as –OH (**8** and **9**), –NH$_2$(**7** and **10**), and –OMe (**11**) decreased the *c*Log*P*, and addition of more hydrophobic ones such as –Me (**12**) and –Cl (**13**) increased the *c*Log*P*. However, adding –NH$_2$ groups, which had the most beneficial effect on *c*Log*P*, also increased markers of toxicity (Table 2) and, except for addition at the 5 position (Compound **10**), reduced the EF inhibitory activity.

Adding functional groups such as –OH (**8**, **9** and **14**), –Me (**12** and **15**), and –Cl (**13**) at *ortho* (2 or 6) positions to the carboxyl group (or ester) reduced the expected toxicities, with acceptable binding energies. However, they also affected the IC_{50} values, depending on the groups and their positions. Electron donating groups on carbons 2, 4 and 6 (e.g., –OH) should increase the electron density on the oxygen atoms of the carboxyl group or the ester, which can enhance interactions between the ligands and receptor. However, these additions may also reduce interactions with active site residues by increasing desolvation energies.

Positional effects may be explained by how the additional groups affect the ability of the carboxyl group (or a carboxy methyl ester) to interact with metal ions in the active site. For example, adding –OH at position 6 of **5** (compound **14**) renders it completely inactive, while additions at the 2 and 4 positions (compounds **15** and **16**) did not decrease activity significantly. This may be because interaction between the sp^2 oxygen atom of the ester of **14** and the

metal ion was decreased by an intramolecular hydrogen bond between the –OH and the sp^2 oxygen atom. This effect would not be anticipated in compound **8**, as both oxygen atoms of the carboxyl group are strong hydrogen bond acceptors, and an intramolecular hydrogen bond between the –OH and one oxygen atom should have little effect on the interaction of the other oxygen atom with the metal ion. Electron withdrawing groups (e.g., Cl) would be expected to decrease the electron density of the oxygen atoms of the carboxyl group or the ester, thus reducing interactions between the ligands and receptors. Adding a methyl group, a hydrophobic and weak electron donating group, to the *ortho* positions to the carboxyl group (or ester) (e.g., compare **12** with **1** and **15** with **5**) did not improve activity, and raised the *c*Log*P* considerably.

2.4. Effect of changing the carboxyl group to other functional groups

Changing the carboxyl group of **1** and its derivatives to methyl esters (**14–16**) reduced the expected toxicities but increased *c*Log*P* values. The reduction in potencies could be due to reduced interactions of the less Lewis basic oxygen atoms of the esters with the metal ions in the active site. In **14**, as in **9**, adding an additional 6-OH group rendered the compound inactive.

While a group is necessary at the 1 position (compound **4** is relatively inactive), substitutions of the carboxyl group of **1** with groups having weaker hydrogen bond forming abilities yielded the most promising derivatives in this study. For example, adding –SMe (**17**) reduced activity, but addition of –OCF$_3$ (**18**), –NMe$_2$ (**19**) and –Cl (**20**) all gave inhibitory activities similar to those of Compound **1**. The latter groups are much weaker hydrogen bond donors than –SMe. The overall ability of compounds **18–20** to inhibit may thus be due to their more favorable desolvation energies. The relatively low activity of **21** might be attributable to the hydrophilic group C(O)NHOH being a weaker hydrogen bond donor than the carboxyl group.

Substituting the carboxyl with the hydrogen bond donor group 3-carbamimidoyl, –C(=NH)NH$_2$, (**22**) yielded a compound with a reduced *c*Log*P*, and better than or equivalent activity to **1** in the bioassay. Docking of both the neutral (–C(=NH)NH$_2$) and the positively charged (–C=NH$_2$NH$_2$$^+$) forms of **22** to 1K90 (Fig. 3) suggested that this group could make strong hydrogen bonds with the backbone oxygen atoms from the active site residues of Lys346, Gly347, Val350 and the carboxyl group of Asp491. As **22**

has no toxicity markers, it was selected to start further testing as the next generation of EF inhibitor.

3. Discussion

Although early treatment with antibiotics can greatly reduce the effects of bacterial infections, inhibitors of the toxins could play a therapeutic role in later stage infections and in preventing diarrhea or death, based on the type of infection. Our previously identified lead compound **1** was active in bioassays in the low μM range, and the effective dose to reduce diarrhea in mice (from ETEC) was also low, on the order of 7.5–15 μg when given intraperitoneally or by gavage.[8] Before beginning additional animal studies, it was necessary to eliminate as many markers of toxicity as possible, and improve solubility. Our goals in this study were to optimize activity, by designing compounds to retain biological activity while improving pharmaceutically important properties, such as solubility, and to remove known markers of toxicity or mutagenicity (properties summarized in Tables 1 and 2). These compounds would allow us to proceed to more advanced animal trials for inhibiting anthrax in the rabbit model.[22] Also, in light of recent outbreaks of *E. coli*, for example in Germany,[23] a variety of compounds with similar activities to our Compound **1** should be available for testing against other toxin producing *E. coli* strains. Our initial results indicated that the fluorenone ring contributed to the inhibitory activity, and thus, we focused this study on the benzoic acid side chain, which had some markers of toxicity (Table 2).

3.1. The importance of the fluorenone for activity

Compound, **1** was chosen as our lead compound as it consistently scored very high in all our library dockings, and proved the most soluble of all three lead compounds we obtained from our preliminary screenings.[6] In these dockings, the fluorenone ring overlaid the position of the adenine ring of 3d′-ATP in the crystal structure of EF, much as other large planar inhibitors fit the ATP binding pockets.[24] The fluorenone could not be replaced with smaller rings (Compounds **2** and **3**), suggesting its size and planarity were important. The carbonyl group on the fluorenone ring might be more essential for solubility than activity. Removal (compound **2**) decreased the potency, when compared to compound **5**. However, as this introduced one more rotatable bond than
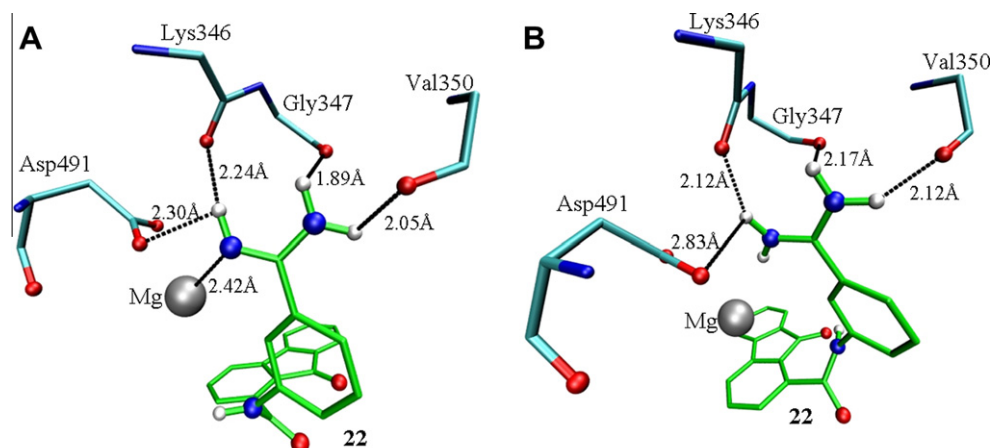
Figure 3. Effect of protonation state of the benzene side chain side chain –C(=NH)NH$_2$ on potential interactions with EF residues. Docking poses are shown for **22** when neutral (A) or positively charged (B). In A, this group interacts with the metal ion, the backbone oxygen atom of Lys346, Gly347, Val50 and the carboxyl group of Asp491, while in B it interacts with the backbone oxygen atoms of Lys346, Gly347, Val50 and the carboxyl group of Asp491.

compound **5**, this would result in a predicted free energy cost for rotor restrictions of about 3.5–5.0 kJ/mol per rotor.[25] This additional rotation should increase the IC_{50} value considerably, and this alone should increase the IC_{50} 4.1–7.5 times.

Both hydrogen bond acceptors and hydrogen bond donors on the benzene ring improved the predicted $c\,Log\,P$, without changing activity. Substitutions at the benzoic acid affected the optimal docking conformation of closely related compounds on EF, suggesting that there are many ways that these compounds could bind within the active site and still serve as inhibitors. We initially assumed that the carboxyl group was essential, as the docked conformation indicated it interacted with the metal ion and/or positively charged residues such as Arg329, Lys346, Lys353, and Lys372 in the active site, similar to the phosphate oxygens of 3d′-ATP in the crystal structure (which it overlaid). Methoxy analogues in general did not have as high an inhibitory activity as their carboxyl-counterparts, which seemed to confirm the need for a hydrophilic, metal ion binding group. Thus it was surprising that the carboxyl group of the benzoic acid could be exchanged with one that had a much lower affinity for metal ions, 3-carbamimidoyl-phenyl, without losing activity (compound **22** in Table 1). Dockings indicated this inhibitor could target other areas of the active site and might simply better fill the substrate-binding area than the smaller carboxyl group. The dockings also suggested the hydrogen atoms of the group interacted with the backbone oxygen atoms from the residues of Lys346, Gly347, Val350 and carboxyl group of Asp491(Fig. 3).

3.2. Further analysis of the docked conformation suggested other changes that could lead to a more active molecule

The docked conformations of the compounds we tested showed strong binding to three regions of the active site, which are circled in Figure 4. The first is the positively charged region (blue circle) which includes the metal ion and four conserved positively charged residues (Arg329, Lys346, Lys353, and Lys372) that interact with the triphosphate group of 3d′-ATP in the 1K90 crystal structure. The second is the hydrophobic region (green circle)

Figure 4. Schematic drawing, showing the position of 3′dATP (thick ball and stick figure) in the 1K90 crystal structure, overlaid with the docking pose of **22** (green thin ball and stick figure). The silver point indicates the position of the metal ion, the blue and red points indicate positive and negative charged groups, respectively, from EF side chains or backbone oxygens. The blue circle (top left) indicates a positively charged region, where negatively charged groups, for example, the triphosphate of ATP, could be added to enhance inhibitory activity. The red circle (top right) indicates a negatively charged region formed by the backbone oxygen atoms of Lys346, Gly347 Val350 and the carboxyl group of Asp491, where the –C(=NH)NH₂ side chain of the 3-carbamimidoylphenyl group of **22** lies. The Green circle (bottom) indicates a hydrophobic region formed by the side chains of Leu348, and other residues that are not explicitly shown, where the purine of ATP and the fluorenone of **22** lie.

formed by the apolar hydrogen and carbon atoms from the side chain of Leu348, Asn583, Gly547, etc, where the purine of 3d′ATP is located in the 1K90 structure, and the fluorenone in the docked structures of all derivatives is located. The third, negatively-charged region (red circle) includes the backbone oxygen atoms from the residues of Lys346, Gly347, Val350 and the carboxyl group of Asp491. The –C(=NH)NH₂ of **22** could form hydrogen bonds with EF in this last region, thus accounting for its relatively good activity. This structure–activity analysis, following traditional approaches,[26–28] suggests that activity could be further improved by adding both hydrogen bond acceptors and hydrogen bond donors to the benzene ring so that the ligands could interact with positively-charged residues and negatively-charged backbone oxygen atoms. Adding both hydrogen bond acceptors and hydrogen bond donors to the benzene ring could increase the activity, as illustrated by **10**, which was among the most active compounds. Docking suggested that the negatively charged carboxyl group can interact with positively charged residues, while the amino group –NH₂, in its protonated form, interacts with the negatively charged region. The activity of **1** would also be improved by changing its carboxyl group to even larger hydrogen bond acceptors and/or negatively-charged groups, to fully occupy the positively-charged region (blue circle in Fig 4). A single carboxyl group could not occupy this region as effectively as the tri-phosphate group of ATP (thick lines).
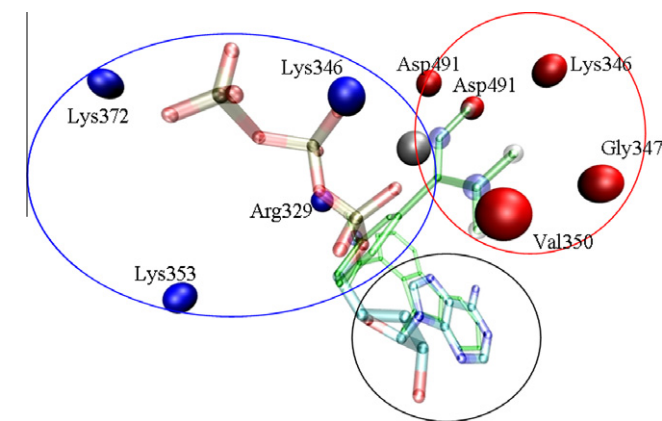
3.3. Docking scores do not directly correlate with EF-inhibitory activity, especially when the ligands can adopt multiple protonated states

The results in Table 1 show that there is no direct relationship between docking scores and activities, although compound **10**, which had the best activity of the series, also had the lowest docking energy. However, compound **6** had a similarly low docking energy, but was inactive (as discussed in Section 2.2). An additional factor in docking is the need to account for variable protonation states of ligands, as we previously discussed.[5] For example, the active compounds **10**, and **19** have basic groups that can be protonated, allowing their interaction with negatively charged residues in the active site (red circle in Fig. 4). Other reasons are that the scoring functions of AutoDock does not fully consider the desolvation energies of ligands binding to the active site, and that flexible side chain interactions were not considered in our dockings. A final complicating factor in our bioassay is possible interactions with media or cellular components.

3.4. Optimization must take into account potential toxicity and balance interactions with the solvent and within the active site

As noted at the outset, we modified compound **1** as it proved to have some mutagenic potential in the Genescreen assay. As this toxicity was consistent with predictions from the Osiris property predictor (Table 2), we also used these predictions to eliminate some active derivatives. Compounds **10** and **19**, while among the more active compounds in inhibiting EF, were rejected based on their high mutagenic and irritant potential, although neither caused obvious toxicity to the cultured cells.

One other result of our SAR analysis was the need to balance adding charged groups to increase ligand-receptor hydrogen bonds, which also decreased the favorable desolvation energies obtained from binding of a more hydrophobic molecule. This fact may account for the basic ability of **1** (with a $c\,Log\,P$ of 4) to inhibit ATP (which has a $c\,Log\,P$ of about −8) from binding to the active site of EF: while the tri-phosphate group of ATP probably interacts better with the metal ion and active site positively charged residues, its low $c\,Log\,P$ and high negative charge (−4) would indicate an

unfavorable net desolvation energy. It may also explain why derivatives of **1** with two carboxyl groups on the benzene ring had reduced activity (data not shown). Further redesign of this molecule will need to take such tradeoffs into account.

4. Conclusions

Modifying the benzoic acid ring of the lead compound **1** produced two compounds (**8** and **22**) with improved or similar inhibition of EF affects on cultured cells, increased aqueous solubility and reduced expected toxicities. The switch from a hydrogen-bond donor group (–COOH) to a hydrogen-bond acceptor group (–C(=NH)NH₂) produced the most promising compound, **22**, when aqueous solubility ($c\log P$) and low potential toxicity is weighted above the other evaluation criteria. To further improve **22** binding to the three regions in the active site of EF, one could test the effects of adding additional hydrogen bond acceptors or electron-donating groups to the benzimidamide ring of **22**.

5. Experimental Section

5.1. Synthesis

5.1.1. General procedure for the amide coupling

In a reaction vessel, the corresponding carboxylic acids (0.91 mmol) were dissolved in CH_3CN (10 mL), then BOP (1 mmol, 442 mg, 1.1 equiv) was added followed by diisopropyl ethyl amine (DIPEA) (2.73 mmol, 0.47 ml, 3.0 equiv). Upon addition of DIPEA the mixture became a homogeneous solution. After 5 min stirring at room temperature the relevant amines (1 mmol, 1.1 equiv) were added. The reaction was monitored by TLC and LCMS (1 hr to overnight) and elevated temperature was used when necessary. Upon completion, the product precipitated out. The precipitates were filtered and washed with CH_2Cl_2, H_2O, affording the desired products in moderate to good yields (55–92%). All compounds were purified to >95% as assessed by HPLC.

5.1.2. General procedure for the methyl ester cleavage

To a reaction vessel containing the corresponding methyl esters (0.5 mmol) in 30 mL of THF–H₂O (2:1 ratio) was added LiOH·H₂O (1.5 mmol, 3 equiv). The mixture was refluxed overnight. Upon completion, monitored by TLC, the solvent was evaporated; the mixture was diluted in CH_2Cl_2 and acidified with 0.5 M HCl until pH 2. The precipitated solid was then filtered and washed with CH_2Cl_2, H_2O affording the acid in good yields (75–99%).

5.1.3. General procedure for the acid chloride formation

To a dried and tared 50 mL round bottom reaction flask equipped with a stirring bar was added 3-[(9-oxo-9H-fluorene-1-carbonyl)-amino]-benzoic acid (16 mmol, 3.59 g) and thionyl chloride (20 ml). The mixture was refluxed 3 h. Upon completion, monitored by TLC, the thionyl chloride was removed by distillation. The resulting solid was dried overnight under vacuum to remove trace amounts of thionyl chloride, affording the crude acid chloride in good yields (91–98%).

5.1.4. General procedure for the amide bond formation via acid chloride

To a stirred solution of amine (1.1 mmol, 1.1 equiv) and 0.46 mL triethylamine (3.3 mmol, dissolved in 2 mL dry CH_2Cl_2 at 0 °C, was added dropwise a solution of acid chloride (1 mmol, 1 equiv) in 2 mL dry CH_2Cl_2. Stirring was continued at 0 °C for 1 h and at room temperature for 3 h. The reaction mixture was diluted with 2–5 mL CH_2Cl_2, and acidified by 2 N HCl until pH 4. The precipitate was filtered, washed with H_2O, CH_2Cl_2, and dried to give moderate-to-good yields (64–95%).

5.1.5. 3-(9-Oxo-9H-fluorene-1-carboxamido)benzoic acid (1)

Synthesized from methyl 3-(9-oxo-9H-fluorene-1-carboxamido)benzoate according to the general procedure described above for ester cleavage. Yield 98%. ¹H NMR (DMSO-d_6, 300 MHz): δ 13.00 (br, 1H), 10.69 (s, 1H), 8.34 (t, J = 1.8 Hz, 1H), 7.85–7.96 (m, 3H), 7.70 (t, J = 7.7 Hz, 2H), 7.61–7.64 (m, 2H), 7.52 (dd, J = 6.6, 0.8 Hz, 1H), 7.48 (t, J = 7.7 Hz, 1H), 7.41 (t, J = 7.5 Hz, 1H). LCMS m/z [M+1] 343.08 .

5.1.6. 3-[(Biphenyl-3-carbonyl)-amino]-benzoic acid (2)

To a microwave vessel containing 3-[(biphenyl-3-carbonyl)-amino]-benzoic acid methyl ester (1.0 equiv, 55 mg, 0.17 mmol) in 5 ml of THF–H₂O (3:1) was added LiOH (6.0 equiv, 43 mg, 1.02 mmol). The mixture was allowed to warm to 60 °C for 1.5 h. Upon reaction completion, the solvent was evaporated and the aqueous layers were acidified with 0.5 M HCl. The white precipitate was washed with cold water yielding the product in 43% yield. ¹H NMR (DMSO, 300 MHz): δ 12.98 (bs, 1H), 10.49 (s, 1H), 8.40 (t, J = 2.3 Hz, 1H), 8.24 (t, J = 2.3 Hz, 1H), 8.08–8.05 (m, 1H), 7.95 (bd, J = 7.7 Hz, 1H), 7.88 (bd, J = 7.7 Hz, 1H), 7.77 (d, J = 6.8 Hz, 2H), 7.69–7.59 (m, 2H), 7.53–7.38 (m, 4H). LCMS m/z [M+1] 317.11.

5.1.7. 3-Benzoylamino-benzoic acid (3)

Synthesized from the corresponding methyl ester according to the general procedure described above for ester cleavage. Yield 50%. ¹H NMR (MeOD, 300 MHz): δ 8.36 (t, J = 1.7 Hz, 1H), 7.97 (dd, J = 2.2, 1.1 Hz, 2H), 7.95–7.92 (m, 2H), 7.80 (dt, J = 7.7, 1.4 Hz, 1H), 7.61–7.43 (m, 5H). LCMS m/z [M+1] 242.02.

5.1.8. 9-Oxo-N-phenyl-9H-fluorene-1-carboxamide (4)

Synthesized from 9-fluorenone-1-carboxilic acid and aniline according to the general procedure describe above for amide coupling. Yield 68%. ¹H NMR (DMSO-d_6, 300 MHz): δ 10.52 (s, 1H), 7.43 (d, J = 7.5 Hz, 1H), 7.86 (d, J = 7.2 Hz, 1H), 7.60–7.71 (m, 5H), 7.51 (d, J = 7.7 Hz, 1H), 7.32–7.43 (m, 3H), 7.10 (t, J = 7.2 Hz, 1H). ¹³C NMR (CDCl₃, 75 MHz): δ 196.2, 161.5, 145.6, 143.5, 138.7, 136.0, 135.3, 134.9, 132.9, 132.6, 129.9, 129.6, 128.9, 125.2, 124.2, 123.2, 120.5, 120.1. LCMS m/z [M+1] 300.09.

5.1.9. Methyl 3-(9-oxo-9H-fluorene-1-carboxamido)benzoate (5)

Synthesized from 9-fluorenone-1-carboxilic acid and the corresponding amine according to the general procedure described above for amide coupling. Yield 91%. ¹H NMR (DMSO-d_6, 300 MHz): δ 10.72 (s, 1H), 8.39 (d, J = 1.8 Hz, 1H), 7.94 (t, J = 7.3 Hz, 2H), 7.88 (dd, J = 7.3, 0.8 Hz, 1H), 7.50–7.76 (m, 6H), 7.42 (t, J = 7.3 Hz, 1H), 3.88 (s, 3H). LCMS m/z [M+1] 357.73.

5.1.10. 5-Amino-2-(9-oxo-9H-fluorene-1-carboxamido)benzoic acid (6)

Synthesized from 9-oxo-9H-fluorene-1-carbonyl chloride and the corresponding amine according to the procedure described above for the amide coupling via acid chloride. A small amount of product was dissolved in DMSO and purified by reverse-phase HPLC (Vydac C18, UV 254) with a linear gradient of 0–100% acetonitrile (0.1% TFA) over 30 min at 4 mL/min. Relevant fractions were combined, and the solvent was removed by freeze-drying to afford the desired product in 15% yield. ¹H NMR (DMSO-d_6, 300 MHz): δ 11.13 (s, 1H), 8.27 (d, J = 8.8 Hz, 1H), 7.94 (d, J = 8.7 Hz, 1H), 7.86 (d, J = 7.7 Hz, 1H), 7.58–7.73 (m, 3H), 7.51 (d, J = 7.7 Hz, 1H), 7.40 (td, J = 7.3, 0.8 Hz, 1H), 7.29 (d, J = 2.2 Hz, 1H), 6.93 (d, J = 7.3 Hz, 1H). LCMS: m/z [M+1] 359.17.

5.1.11. 2-Amino-5-(9-oxo-9H-fluorene-1-carboxamido)benzoic acid (7)

Synthesized from 9-fluorenone-1-carboxilic chloride and the corresponding amine according to the procedure for amide coupling via acid chloride described above. A small amount of product was dissolved in DMSO and purified by reverse-phase HPLC (Vydac C18, UV 254) with a linear gradient of 0–100% acetonitrile (0.1% TFA) over 30 min at 4 mL/min. Relevant fractions were combined, and the solvent was removed by freeze-drying to afford the desired product in 8% yield. ^{1}H NMR (DMSO-d_6, 300 MHz): δ 10.28 (s, 1H), 8.27 (d, $J = 8.8$ Hz, 1H), 7.94 (d, $J = 8.7$ Hz, 1H), 7.86 (d, $J = 7.7$ Hz, 1H), 7.58–7.73 (m, 3H), 7.51 (d, $J = 7.7$ Hz, 1H), 7.40 (td, $J = 7.3$, 0.8 Hz, 1H), 7.29 (d, $J = 2.2$ Hz, 1H), 6.93 (d, $J = 7.3$ Hz, 1H). LCMS m/z [M+1] 359.18.

5.1.12. 2-Hydroxy-3-(9-oxo-9H-fluorene-1-carboxamido)benzoic acid (8)

Synthesized from 9-fluorenone-1-carboxilic chloride and the corresponding amine according to the general procedure describe above for amide coupling via acid chloride. Yield 95%. ^{1}H NMR (DMSO-d_6, 300 MHz): δ 10.52 (s, 1H), 8.33 (dd, $J = 7.7$, 1.1 Hz, 1H), 7.50 (dd, $J = 7.0$, 1.5 Hz, 1H), 7.85 (d, $J = 7.3$ Hz, 1H), 7.59–7.70 (m, 5H), 7.40 (t, $J = 7.3$ Hz, 1H), 6.95 (t, $J = 8.1$ Hz, 1H). LCMS m/z [M+1] 360.10.

5.1.13. 2-Hydroxy-5-(9-oxo-9H-fluorene-1-carboxamido)benzoic acid (9)

Synthesized from the corresponding methyl ester according to the general procedure described above for ester cleavage. Yield 99%. ^{1}H NMR (DMSO-d_6, 300 MHz): δ 10.47 (s, 1H), 8.22 (d, $J = 2.6$ Hz, 1H), 7.93 (d, $J = 7.7$ Hz, 1H), 7.86 (d, $J = 7.3$ Hz, 1H), 7.60–7.77 (m, 4H), 7.50 (d, $J = 6.6$ Hz, 1H), 7.42 (t, $J = 7.3$ Hz, 1H), 6.96 (d, $J = 8.2$ Hz, 1H), 5.74 (s, 1H). LCMS m/z [M+1] 360.09.

5.1.14. 3-Amino-5-(9-oxo-9H-fluorene-1-carboxamido)benzoic acid (10)

Synthesized from 9-oxo-9H-fluorene-1-carbonyl chloride and the corresponding amine according to the procedure described above for the amide coupling via acid chloride. Yield 85%. ^{1}H NMR (DMSO-d_6, 300 MHz): δ 10.76 (s, 1H), 8.37 (s, 1H), 8.12 (d, $J = 2.2$ Hz, 1H), 7.94 (d, $J = 7.3$ Hz, 1H), 7.87 (d, $J = 7.0$ Hz, 1H), 7.62–7.73 (m, 4H), 7.53 (d, $J = 7.7$ Hz, 1H), 7.41 (t, $J = 7.7$ Hz, 1H). LC–MS (ESI): mass calcd for ($C_{21}H_{14}N_2O_4$), m/z 358.10; measured [M+H]$^+$ m/z 359.18.

5.1.15. 4-Methoxy-3-(9-oxo-9H-fluorene-1-carboxamido)benzoic acid (11)

Synthesized from the corresponding methyl ester according to the general procedure described above for ester cleavage. Yield 75%. ^{1}H NMR (DMSO-d_6, 300 MHz): δ 12.72 (br, 1H),10.44 (s, 1H), 8.77 (d, $J = 1.8$ Hz, 1H), 7.95 (d, $J = 7.3$ Hz, 1H), 7.86 (d, $J = 7.3$ Hz, 1H), 7.77 (dd, $J = 8.4$, 1.9 Hz, 1H), 7.62–7.73 (m, 4H), 7.41 (t, $J = 7.5$ Hz, 1H), 7.17 (d, $J = 8.5$ Hz, 1H), 3.91 (s, 3H). LCMS m/z [M+1] 374.13.

5.1.16. 2-Methyl-3-(9-oxo-9H-fluorene-1-carboxamido)benzoic acid (12)

Synthesized from the corresponding methyl ester according to the general procedure described above for ester cleavage. Yield 94%. ^{1}H NMR (DMSO-d_6, 300 MHz): δ 10.17 (s, 1H), 7.92 (d, $J = 7.3$ Hz, 1H), 7.85 (d, $J = 8.1$ Hz, 1H), 7.58–7.71 (m, 4H), 7.51 (d, $J = 7.7$ Hz, 1H), 7.40 (t, $J = 7.2$ Hz, 1H), 7.31 (t, $J = 7.6$ Hz, 1H), 2.44 (s, 3H). LCMS m/z [M+1] 358.14.

5.1.17. 2-Chloro-3-(9-oxo-9H-fluorene-1-carboxamido)benzoic acid (13)

Synthesized from 9-oxo-9H-fluorene-1-carbonyl chloride and the corresponding amine according to the procedure described above for the amide coupling via acid chloride. Yield 80%. ^{1}H NMR (DMSO-d_6, 300 MHz): δ 10.50 (s, 1H), 7.96 (t, $J = 6.9$ Hz, 2H), 7.86 (d, $J = 7.4$ Hz, 1H), 7.39–7.73 (m, 7H). LCMS m/z [M+1] 378.08.

5.1.18. Methyl 2-hydroxy-5-(9-oxo-9H-fluorene-1-carboxamido)benzoate (14)

Synthesized from 9-fluorenone-1-carboxilic acid and the corresponding amine according to the general procedure described above for amide coupling. Yield 72%. ^{1}H NMR (DMSO-d_6, 300 MHz): δ 10.48 (s, 1H), 8.24 (d, $J = 2.4$ Hz, 1H), 7.92 (d, $J = 7.4$ Hz, 1H), 7.85 (d, $J = 7.5$ Hz, 1H), 7.60–7.74 (m, 4H), 7.48 (d, $J = 7.4$ Hz, 1H), 7.40 (t, $J = 7.4$ Hz, 1H), 6.99 (d, $J = 8.8$ Hz, 1H), 5.73 (s, 1H), 3.91 (s, 3H). LCMS m/z [M+1] 374.12.

5.1.19. Methyl 2-methyl-3-(9-oxo-9H-fluorene-1-carboxamido)benzoate (15)

Synthesized from 9-fluorenone-1-carboxilic acid and the corresponding amine according to the general procedure described above for amide coupling. Yield 80%. ^{1}H NMR (DMSO-d_6, 300 MHz): δ 10.24 (s, 1H), 7.89 (dd, $J = 10.6$, 7.7 Hz, 3H), 7.62–7.75 (m, 4H), 7.51 (d, $J = 7.7$ Hz, 1H), 7.41 (m, 2H), 3.85 (s, 3H), 2.44 (s, 3H). LCMS m/z [M+1] 371.98.

5.1.20. Methyl 4-methoxy-3-(9-oxo-9H-fluorene-1-carboxamido)benzoate (16)

Synthesized from 9-fluorenone-1-carboxilic acid and the corresponding amine according to the general procedure described above for amide coupling. Yield 90%. ^{1}H NMR (DMSO-d_6, 300 MHz): δ 10.50 (s, 1H), 8.81 (d, $J = 1.8$ Hz, 1H), 7.95 (dd, $J = 7.2$, 1.1 Hz, 1H), 7.86 (d, $J = 7.5$ Hz, 1H), 7.80 (dd, $J = 8.5$, 2.2 Hz, 1H), 7.62–7.73 (m, 4H), 7.40 (td, $J = 7.5$, 1.0 Hz, 1H), 7.21 (d, $J = 8.6$ Hz, 1H), 3.92 (s, 3H), 3.86 (s, 3H). LCMS m/z [M+1] 388.15.

5.1.21. N-(3-(methylthio)phenyl)-9-oxo-9H-fluorene-1-carboxamide(17)

Synthesized from 9-fluorenone-1-carboxilic acid and the corresponding amine according to the general procedure described above for amide coupling. Yield 92%. ^{1}H NMR (DMSO-d_6, 300 MHz): δ 10.53 (s, 1H), 7.94 (dd, $J = 7.4$ Hz, 0.8 Hz, 1H), 7.86 (d, $J = 7.4$ Hz, 1H), 7.06–7.72 (m, 4H), 7.39–7.51 (m, 3H), 7.30 (t, $J = 7.7$ Hz, 1H), 7.00 (dt, $J = 7.7$, 0.8 Hz, 1H), 2.48 (s, 3H). LCMS m/z [M+1] 346.11.

5.1.22. 9-Oxo-N-(3-(trifluoromethoxy)phenyl)-9H-fluorene-1-carboxamide (18)

Synthesized from 9-fluorenone-1-carboxilic acid and the corresponding amine according to the general procedure described above for amide coupling. Yield 77%. ^{1}H NMR (DMSO-d_6, 300 MHz): δ 10.77 (s, 1H), 7.94 (d, $J = 7.4$ Hz, 1H), 7.86 (d, $J = 7.2$ Hz, 2H), 7.56–7.72 (m, 4H), 7.38–7.51 (m, 3H), 7.10 (d, $J = 8.0$ Hz, 1H). LCMS m/z [M+1] 384.01.

5.1.23. N-(3-(dimethylamino)phenyl)-9-oxo-9H-fluorene-1-carboxamide (19)

Synthesized from 9-fluorenone-1-carboxilic acid and the corresponding amine according to the general procedure described above for amide coupling. Yield 85%. ^{1}H NMR (DMSO-d_6, 300 MHz): δ 10.36 (s, 1H), 7.92 (d, $J = 6.9$ Hz, 1H), 7.86 (d, $J = 7.2$ Hz, 1H), 7.60–7.71 (m, 3H), 7.50 (d, $J = 7.7$ Hz, 1H), 7.40 (t, $J = 7.4$ Hz, 1H), 7.02–7.17 (m, 3H), 6.49 (dd, $J = 7.8$, 2.2 Hz, 1H), 2.90 (s, 6H). LCMS m/z [M+1] 343.17.

5.1.24. N-(3-chloro-4-fluorophenyl)-9-oxo-9H-fluorene-1-carboxamide (20)

Synthesized from 9-fluorenone-1-carboxilic acid and the corresponding amine according to the general procedure described above for amide coupling. Yield 91%. ^{1}H NMR (DMSO-d_6, 300 MHz): δ 10.70 (s, 1H), 8.00 (dd, $J = 6.8$, 2.5 Hz, 1H), 7.95 (d, $J = 7.4$ Hz, 1H), 7.86 (d, $J = 7.4$ Hz, 1H), 7.23–7.55 (m, 4H), 7.38–7.51 (m, 3H). LCMS m/z [M+1] 351.98.

5.1.25. N-(3-(hydroxycarbamoyl)phenyl)-9-oxo-9H-fluorene-1-carboxamide (21)

To a 50 ml round bottom flask was added methyl 3-(9-oxo-9H-fluorene-1-carboxamido)benzoate (0.05 mmol, 17.87 mg, 1 equiv), hydroxylamine hydrochloride (0.4 mmol, 28 mg, 8 equiv) and 20 mL MeOH. After the dropwise addition of KOH/MeOH (1 M, 0.5 mL), the mixture was refluxed overnight. Upon reaction completion monitored by TLC, the methanol was evaporated. The mixture was diluted in $CHCl_3$ and yellow hydrolyzed products precipitated. After filtration, the filtrate was collected and the crude product was purified by chromatography (1% MeOH/CHCl$_3$) to give the desired product as white solid in 78% yields. ^{1}H NMR (DMSO-d_6, 300 MHz): δ 12.59 (s, 1H), 10.70 (s, 1H), 8.48 (t, $J = 1.6$ Hz, 1H), 8.35 (d, $J = 7.3$ Hz, 1H), 7.89–7.98 (m, 3H), 7.67 (dt, $J = 7.7$, 1.4 Hz, 1H), 7.38–7.54 (m, 5H). LCMS m/z [M+15] 373.17.

5.1.26. N-(3-carbamimidoylphenyl)-9-oxo-9H-fluorene-1-carboxamide (22)

Synthesized from 9-fluorenone-1-carboxilic acid and the corresponding amine according to the general procedure described above for amide coupling. Upon reaction completion, the reaction solvent was evaporated and CH_2Cl_2 was added. The mixture was acidified by 2 N HCl. Then the water layer was separated and sat at room temperature for a certain time during which yellow precipitates formed. The solid was filtered and washed with H_2O, CH_2Cl_2 to give the desired product in 60% yield. ^{1}H NMR (DMSO-d_6, 300 MHz): δ 10.58 (s, 1H), 7.91 (d, $J = 7.3$ Hz, 1H), 7.84 (d, $J = 7.4$ Hz, 1H), 7.57–7.70 (m, 3H), 7.19–7.40 (m, 4H), 6.94 (d, $J = 6.6$ Hz, 1H). LCMS m/z [M+1] 342.16.

5.2. General pAssay for inhibition of EF

Inhibition of EF was done as previously described[6], by treating murine monocyte/macrophage cells (RAW 264.7) with PA (2.5 μg/ml) and EF (0.625 μg/ml) in the presence of DMEM medium or compounds initially dissolved in DMSO and diluted in DMEM (w/o phenol red) containing isobutylmethylxanthine (IBMX). Experiments included controls for DMSO and IBMX. Plates were then incubated for 4 h at 37 °C in 5% CO_2. Following incubation, the culture supernatants were removed and assayed for cAMP with a cAMP-specific ELISA from Assay Designs, Inc. (Ann Arbor, Michigan) per manufacturer directions.

5.3. Assays for toxicity and mutagenicity of Compound 1

(GADD45α-GFP, GreenScreen HC and the AMES IIT Mutagenicity) were performed under Good Laboratory Practice (GLP) by BioReliance (Rockville, MD).[29] The genotoxicity potential of 1 was assessed using the Green Screen HC [GADD45α-GFP [Human Cells (HC) GADD45α (growth arrest and DNA damage gene)-Green Fluorescent Protein (GFP) assay from Gentronix© in a high throughput 96 well plate format. The assay links the regulation of the human GADD45α gene to the production of GFP to indicate the genotoxic potential. Two human cell lines, GenM-C01 and GenM-T01 (Gentronix©, Manchester, UK) were used. The reporter cell line (GenM-T01) consists of TK6 cells transfected by electroporation with an episomally replicating Epstein-Barr virus-based plasmid bearing the upstream promoter region and regulatory genes sequences of the human GADD45α gene operatively linked to a human codon optimized EGFP gene. The control cell line (GenM-C01) is TK6 cells tranfected with an identical plasmid except that 4 bp have been removed at the start of the EGFP gene, such that a functional GFP protein is not produced. The plasmids are stably maintained in TK6 cells by addition of 200 μg/ml hygromycin B to the cultures. Further assay details are included in Supplementary data.

Compound 1 was determined to be non-mutagenic in all conditions tested (Supplementary data Table 1b). All criteria for a valid test were met. Compound 1 was determined to be cytotoxic at 62.5 μg/ml and was determined to have some genotoxic activity at 62.5 μg/ml (Supplementary data Fig. 1 and Table 1a). The positive and negative controls were within expected ranges. Compound 1 had a doubling in the number of revertants in one dose with tester strain TAMix with metabolic activation. There was no dose response trend and the doubling was within historical negative control data range.

5.4. Docking

The lead compound (1) and its derivatives (2–22) were docked to a crystal structure of edema factor 1K90.pdb (resolution 2.75 Å, r-value 0.225) with AutoDock3.0.5. The 'Lamarckian' genetic algorithm (LGA) was used for all docking. The number of iterations was set to 200 and population size to 100. The ligand and solvent molecules were removed from the crystal structure to obtain the docking grid and the active site was defined using AutoGrid. The grid size was set to $90 \times 90 \times 90$ points with grid spacing of 0.375 Å. The grid box was centered on the center of the 3d′ATP from the corresponding crystal structure complexes. The Yb^{3+} ion in the active site coordinates carboxyl groups of residues Asp491, Asp493 and His577 (Yb-N:2.78 Å) and an oxygen atom of the α-phosphate group of the 3′dATP ligand. For all the dockings using the 1K90 crystal structure, Yb^{3+} was replaced with the more physiological Mg^{2+} at the same position, which allowed better comparison of the energy data.

Acknowledgments

Supplementary data

Supplementary data (Table 1a: Greenscreen assay description and results; Table 1b: AmesII mutagenicity assay results; Table 2s: Table 1 reordered according to activity of the compound, illustrating the lack of correlation between absolute docking scores and activity.) associated with this article can be found, in the online version, at doi:10.1016/j.bmc.2011.10.091.

References and notes

1. Migone, T. S.; Subramanian, G. M.; Zhong, J.; Healey, L. M.; Corey, A.; Devalaraja, M.; Lo, L.; Ullrich, S.; Zimmerman, J.; Chen, A.; Lewis, M.; Meister, G.; Gillum, K.; Sanford, D.; Mott, J.; Bolmer, S. D. N. Engl. J. Med. 2009, 361, 135.
2. Sweeney, D. A.; Cui, X.; Solomon, S. B.; Vitberg, D. A.; Migone, T. S.; Scher, D.; Danner, R. L.; Natanson, C.; Subramanian, G. M.; Eichacker, P. Q. J. Infect. Dis. 2010, 202, 1885.
3. Kulshreshtha, P.; Bhatnagar, R. Mol. Immunol. 2011, 48, 1958.
4. Laine, E.; Goncalves, C.; Karst, J. C.; Lesnard, A.; Rault, S.; Tang, W. J.; Malliavin, T. E.; Ladant, D.; Blondel, A. Proc. Natl. Acad. Sci. U.S.A. 2010, 107, 11277.

5. Chen, D. L.; Menche, G.; Power, T. D.; Sower, L.; Peterson, J. W.; Schein, C. H. *Proteins-Struc. Funct. Bioinformatics* **2007**, *67*, 593.
6. Chen, D.; Misra, M.; Sower, L.; Peterson, J. W.; Kellogg, G. E.; Schein, C. H. *Bioorg. Med. Chem.* **2008**, *16*, 7225.
7. Chen, D.; Martin, Z. S.; Soto, C.; Schein, C. H. *Bioorg. Med. Chem.* **2009**, *17*, 5189.
8. Moen, S. T.; Blumentritt, C. A.; Slater, T. M.; Patel, S. D.; Tutt, C. B.; Estrella-Jimenez, M. E.; Pawlik, J.; Sower, L; Popov, V. L.; Schein, C. H.; Gilbertson, S. R.; Peterson, J. W.; Torres, A. G. *Infect. Immun.* **2010**, 78.
9. Chen, D. L.; Schein, C. H. *Abstr. Pap. Am. Chem. S.* **2008**, 235.
10. Roland, K. L.; Cloninger, C.; Kochi, S. K.; Thomas, L. J.; Tinge, S. A.; Rouskey, C.; Killeen, K. P. *Vaccine* **2007**, *25*, 8574.
11. Lasaro, M. A.; Mathias-Santos, C.; Rodrigues, J. F.; Ferreira, L. C. *FEMS Immunol. Med. Microbiol.* **2009**, *55*, 93.
12. Liang, W.; Pascual-Montano, A.; Silva, A. J.; Benitez, J. A. *Microbiology* **2007**, *153*, 2964.
13. Wang, L.; Hashimoto, Y.; Tsao, C. Y.; Valdes, J. J.; Bentley, W. E. *J. Bacteriol.* **2005**, *87*, 2066.
14. Morris, G. M.; Goodsell, D. S.; Halliday, R. S.; Huey, R.; Hart, W. E.; Belew, R. K.; Olson, A. J. *J. Comput. Chem.* **1998**, *19*, 1639.
15. Morris, G. M.; Goodsell, D. S.; Huey, R.; Olson, A. J. *J. Comput. Aided Mol. Des.* **1996**, *10*, 293.
16. Drum, C. L.; Yan, S. Z.; Bard, J.; Shen, Y. Q.; Lu, D.; Soelaiman, S.; Grabarek, Z.; Bohm, A.; Tang, W. J. *Nature* **2002**, *415*, 396.
17. Barth, H.; Aktories, K.; Popoff, M. R.; Stiles, B. G. *Microbiol. Mol. Biol. Rev.* **2004**, *68*, 373.
18. Briggs, C. A.; Schrimpf, M. R.; Anderson, D. J.; Gubbins, E. J.; Grønlien, J. H.; Håkerud, M.; Ween, H.; Thorin-Hagene, K.; Malysz, J.; Li, J.; Bunnelle, W. H.; Gopalakrishnan, M.; Meyer, M. D. *Br. J. Pharmacol.* **2008**, *153*, 1054.
19. Alcaro, S.; Arena, A.; Di Bella, R.; Neri, S.; Ottanà, R.; Ortuso, F.; Pavone, B.; Trincone, A.; Vigorita, M. G. *Bioorg. Med. Chem.* **2005**, *13*, 3371.
20. Murray-Rust, P.; Glusker, J. P. *J. Am. Chem. Soc.* **1984**, *106*, 1018.
21. Wang, R.; Lai, L.; Wang, S. *J. Comput. Aided Mol. Des.* **2002**, *16*, 11.
22. Wycoff, K. L.; Belle, A.; Deppe, D.; Schaefer, L.; Maclean, J. M.; Neuss, S.; Trilling, A. K.; Liu, S.; Leppla, S. H.; Geren, I. N.; Pawlik, J.; Peterson, J. W. *Antimicrob. Agents Chemother.* **2010**.
23. Rasko, D. A.; Webster, D. R.; Sahl, J. W.; Bashir, A.; Boisen, N.; Scheutz, F.; Paxinos, E. E.; Sebra, R.; Chin, C.-S.; Iliopoulos, D.; Klammer, A.; Peluso, P.; Lee, L.; Kislyuk, A. O.; Bullard, J.; Kasarskis, A.; Wang, S.; Eid, J.; Rank, D.; Redman, J. C.; Steyert, S. R.; Frimodt-Møller, J.; Struve, C.; Petersen, A. M.; Krogfelt, K. A.; Nataro, J. P.; Schadt, E. E.; Waldor, M. K. *N. Engl. J. Med.* **2011**, *365*, 709.
24. Bullock, A. N.; Russo, S.; Amos, A.; Pagano, N.; Bregman, H.; Debreczeni, J. É.; Lee, W. H.; Delft, F. v.; Meggers, E.; Knapp, S. *PLoS ONE* **2009**, *4*, e7112.
25. Williams, D. H.; Searle, M. S.; Mackay, J. P.; Gerhard, U.; Maplestone, R. A. *Proc. Natl. Acad. Sci. U.S.A.* **1993**, *90*, 1172.
26. Shuker, S. B.; Hajduk, P. J.; Meadows, R. P.; Fesik, S. W. *Science* **1996**, *274*, 1531.
27. Erlanson, D.; Wells, J.; Braisted, A. *Annu. Rev. Biophys. Biomol. Struct.* **2004**, *33*, 199.
28. Erlanson, D. A.; McDowell, R. S.; O'Brien, T. *J. Med. Chem.* **2004**, *47*, 3463.
29. Hastwell, P. W.; Chai, L. L.; Roberts, K. J.; Webster, T. W.; Harvey, J. S.; Rees, R. W.; Walmsley, R. M. *Mutat. Res.* **2006**, *607*, 160.
30. Compound **1** is referred to in US patent 8,003, 692, (Schein et al., *Methods and Compositions to Inhibit Edema Factor and Adenylyl Cyclase*, **2011**) as FIV-50; it was also called DC-5 in our earlier publications. The names for other compounds are: **4**: FIV-61; **5**: FIV-64; **6**: FIV-72; **7**: FIV-73; **8**: FIV-39; **9**: FIV-35; **10**: FIV-75; **11**: FIV-59; **12**: FIV-55; **13**: FIV-71; **14**: FIV-53; **15**: FIV-54; **16**: FIV-58; **17**: FIV-66; **18**: FIV-67; **19**: FIV-65; **20**: FIV-60; **21**: FIV-46; **22**: FIV-68.